A bidirectional antagonism between aPKC and Yurt regulates epithelial cell polarity

Clémence L. Gamblin,[1,2] Émilie J.-L. Hardy,[1,2] François J.-M. Chartier,[1,2] Nicolas Bisson,[1,2] and Patrick Laprise[1,2]

[1]Département de Biologie Moléculaire, Biochimie Médicale et Pathologie and Centre de Recherche sur le Cancer, Université Laval, and [2]Axe Oncologie, Centre de Recherche du Centre Hospitalier Universitaire de Québec, Québec, Québec G1R 3S3, Canada

During epithelial cell polarization, Yurt (Yrt) is initially confined to the lateral membrane and supports the stability of this membrane domain by repressing the Crumbs-containing apical machinery. At late stages of embryogenesis, the apical recruitment of Yrt restricts the size of the apical membrane. However, the molecular basis sustaining the spatiotemporal dynamics of Yrt remains undefined. In this paper, we report that atypical protein kinase C (aPKC) phosphorylates Yrt to prevent its premature apical localization. A nonphosphorylatable version of Yrt dominantly dismantles the apical domain, showing that its aPKC-mediated exclusion is crucial for epithelial cell polarity. In return, Yrt counteracts aPKC functions to prevent apicalization of the plasma membrane. The ability of Yrt to bind and restrain aPKC signaling is central for its role in polarity, as removal of the aPKC binding site neutralizes Yrt activity. Thus, Yrt and aPKC are involved in a reciprocal antagonistic regulatory loop that contributes to segregation of distinct and mutually exclusive membrane domains in epithelial cells.

Introduction

Epithelial cell polarity is controlled by evolutionarily conserved proteins, including Yurt (Yrt), which contains a 4.1, Ezrin, Radixin, and Moesin (FERM) domain at its N terminus (Hoover and Bryant, 2002; Laprise et al., 2006). FERM domain proteins often play a structural role at the membrane–cytoskeleton interface (Tepass, 2009). Yrt also encloses a FERM adjacent (FA) domain that is found in a subgroup of FERM family members and that is targeted by kinases to modulate the functional properties of these proteins (Baines, 2006). Yrt subcellular distribution is temporally regulated in developing fly embryos. Yrt is initially restricted to the lateral domain and preserves its identity by repressing the activity of apical determinants, including Crumbs (Crb; Laprise et al., 2006, 2009). During terminal differentiation of epithelial tissues, Yrt is recruited apically into the Crb complex and then occupies both lateral and apical domains (Laprise et al., 2006). This correlates with a switch in Yrt functions from a role in global apical–basal polarity to a more specialized local function as an inhibitor of apical membrane growth (Laprise et al., 2006, 2009). Yrt apical localization at late stages of fly embryogenesis correlates with a reduction of its phosphorylation level (Laprise et al., 2006), suggesting that a kinase prevents its premature apical recruitment. The apically localized kinase atypical PKC (aPKC) stands as a prime candidate to fill this role. Indeed, aPKC preserves the identity of the apical membrane through phosphorylation-dependent exclusion of lateral and adherens junction–associated proteins (Betschinger et al., 2003; Plant et al., 2003; Yamanaka et al., 2003; Hutterer et al., 2004; Krahn et al., 2010; Morais-de-Sá et al., 2010; Walther and Pichaud, 2010). In addition, aPKC was shown to phosphorylate Lulu2, which is a mammalian orthologue of Yrt (Hoover and Bryant, 2002; Laprise et al., 2006; Nakajima and Tanoue, 2011). Here, we report that mutually antagonistic interactions between Yrt and aPKC are instrumental for epithelial cell polarity.

Results and discussion

The FA domain of Yrt directly binds to aPKC

To explore the molecular interaction between endogenous aPKC and Yrt, we performed coimmunoprecipitation experiments and found that these proteins formed a complex in *Drosophila melanogaster* embryos (Fig. 1 A). To identify the domain of

Correspondence to Patrick Laprise: Patrick.Laprise@crhdq.ulaval.ca

Abbreviations used in this paper: aPKC, atypical PKC; Crb, Crumbs; *da*, *daughterless*; Dlg, Discs large; FA, FERM adjacent; FERM, 4.1, Ezrin, Radixin, and Moesin; Lgl, Lethal (2) giant larvae; MS, mass spectrometry; UAS, upstream activating sequence; Yrt, Yurt.

The Rockefeller University Press $30.00
J. Cell Biol. Vol. 204 No. 4 487–495
www.jcb.org/cgi/doi/10.1083/jcb.201308032

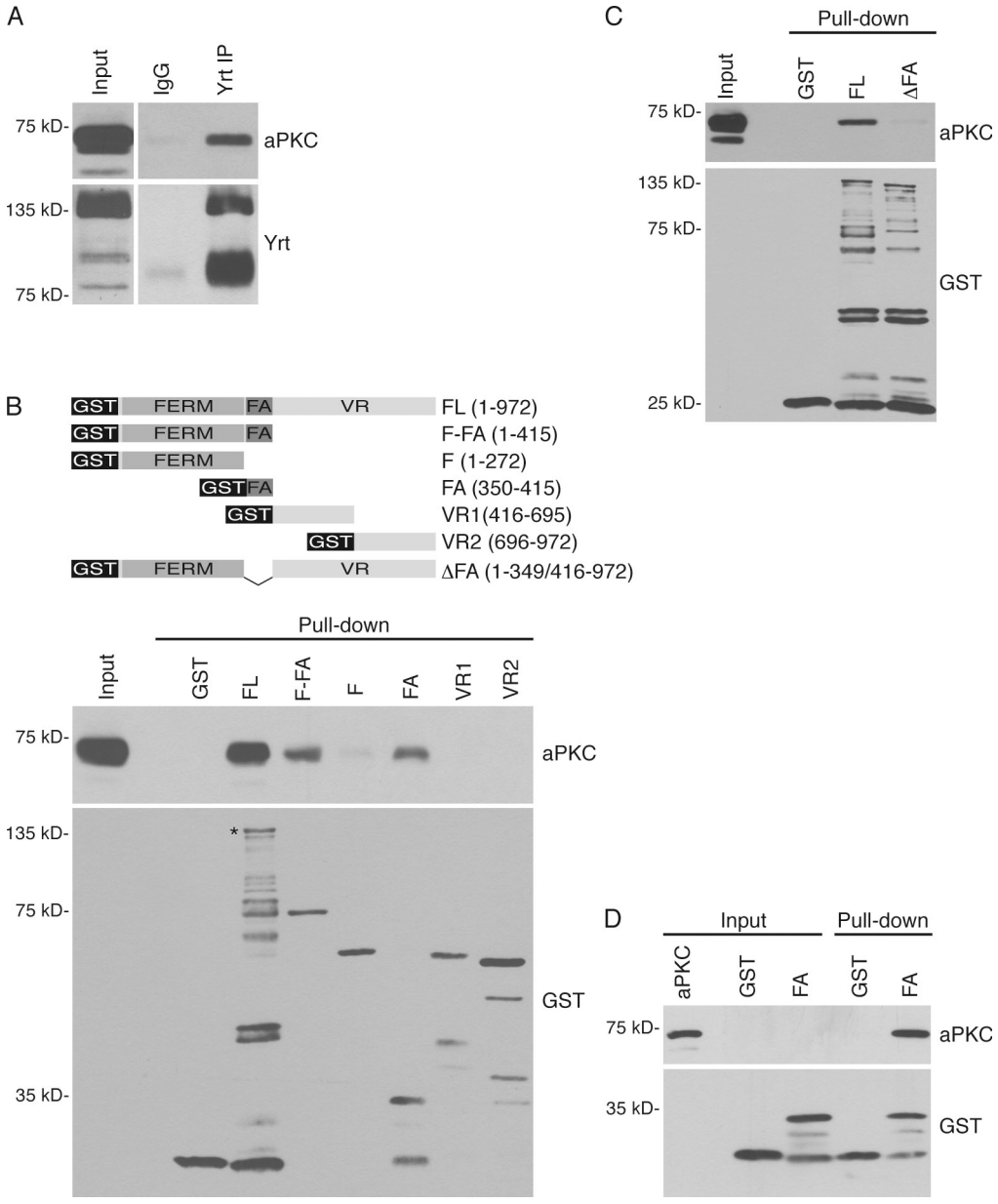

Figure 1. **Yrt directly binds to aPKC via its FA domain.** (A) Endogenous Yrt was immunoprecipitated from a wild-type embryo lysate (Yrt immunoprecipitation [IP]). Guinea pig IgG (IgG) purified from a nonimmune serum was used as a negative control. Western blot using anti-Yrt and anti-aPKC antibodies revealed that the immunoprecipitation was effective and that aPKC coprecipitated with Yrt. A portion of each homogenate was kept to monitor expression of Yrt and aPKC (input). (B and C) Upper portion of Fig. 1 B displays a schematic representation of the GST fusion proteins generated to investigate the Yrt–aPKC interaction. Full-length (FL) Yrt contains a FERM domain at its N terminus followed by a FA domain and a region with no defined domain referred to as the variable region (VR; Laprise et al., 2006). Numbers in brackets indicate the amino acids of Yrt comprised in each construct. GST pull-down experiments were performed on wild-type embryo lysates using these GST chimeric proteins. GST alone was used as a negative pull-down control. Pulled down aPKC was detected by Western blotting, and an anti-GST was used to control the amount of GST or GST fusion proteins used in each experiment. The asterisk indicates full-length Yrt. (D) Purified His-tagged aPKC and GST fused to the FA domain of Yrt (FA) were incubated together, and glutathione-coupled beads were used to pull down the protein complex. Western blotting detected aPKC and controlled the amount of GST or GST-FA used. F, FERM.

Yrt responsible for its association with aPKC, we generated truncated versions of Yrt fused to GST (Fig. 1 B). GST pull-down assays performed on wild-type embryo lysates revealed that the FA domain was sufficient to pull-down aPKC, and removal of this domain strongly reduced the Yrt–aPKC association (Fig. 1, B and C). Residual interaction with aPKC in the absence of the FA domain is likely mediated by the FERM domain, which pulled down a weak but detectable amount of aPKC in contrast to fragments covering the remaining portion of Yrt (Fig. 1 B). The FA domain of Yrt also precipitated purified aPKC (Fig. 1 D), thus demonstrating that their interaction is direct. Collectively, these data define a novel molecular interaction between Yrt and aPKC in *Drosophila* embryos.

aPKC phosphorylates several residues in the FA domain of Yrt

It is plausible that aPKC contributes to Yrt phosphorylation during embryogenesis, as its direct association with Yrt suggests

a kinase–substrate relationship. Accordingly, overexpression of a membrane-targeted form of aPKC (aPKC^{CAAX}) together with its regulator Par-6 (Sotillos et al., 2004; David et al., 2010) increased Yrt phosphorylation at different stages of embryogenesis (Fig. 2 A). Moreover, we observed decreased Yrt phosphorylation levels in *aPKC* mutant embryos compared with their wild-type counterparts (Fig. 2 B). Together, these results demonstrate that Yrt phosphorylation depends on aPKC activity in vivo. To obtain evidence that aPKC directly phosphorylates Yrt, we incubated recombinant full-length Yrt with purified aPKC in presence of radiolabeled ATP and found that Yrt is phosphorylated by aPKC (Fig. 2 C). Of note, the FA domain alone was also efficiently phosphorylated by recombinant aPKC or by endogenous aPKC coprecipitated with Par-6 (Fig. 2, D and E), thus demonstrating that this part of the protein contains critical amino acids targeted by aPKC. This is consistent with the fact that it directly interacts with aPKC (Fig. 1 D) and with previous studies showing that the FA domain of other FERM family members acts as an important phosphorylation-dependent regulatory element (Danilov et al., 1990; Chao and Tao, 1991; Manno et al., 2005; Baines, 2006; Nakajima and Tanoue, 2011). Therefore, we focused our analysis on the FA domain of Yrt, which contains 12 serine/threonine (S/T) residues (Fig. 2 G). aPKC targets four residues in the FA domain of Lulu2 (Fig. 2 G; Nakajima and Tanoue, 2011). Three of these residues are conserved in Yrt (S358, S387, and S392; Fig. 2 G), thus highlighting these amino acids as probable aPKC targets. Mass spectrometry (MS) analysis of Yrt phosphorylated in vitro by aPKC confirmed the phosphorylation of S392 (Fig. S1 A) but not S358 and S387 because of a lack of coverage. Moreover, our MS data identified three additional aPKC phosphorylation sites, namely the evolutionarily conserved S348 and T379 (Nakajima and Tanoue, 2011) as well as S395 (Fig. 2 G and Fig. S1, A–C). Mutation of the five phosphorylated and conserved amino acids (S348, S358, T379, S387, and S392) to alanine residues (A; referred to as the FA^{5A} mutant) strongly suppressed the aPKC-dependent phosphorylation of the FA domain of Yrt, without interfering with its binding to aPKC (Fig. 2, D and F). This shows that we successfully targeted the predominant amino acids that are phosphorylated by aPKC within the FA domain, which contains most aPKC phosphorylation sites within the Yrt sequence (Fig. S2, A–D). Conversion of these five amino acids to aspartate residues (D; FA^{5D}) to generate a phosphomimetic mutant considerably reduced the binding of the FA domain to aPKC (Fig. 2 F). This suggests that Yrt is released from aPKC once phosphorylated, as reported for other aPKC substrates (Yamanaka et al., 2003; Hutterer et al., 2004; Morais-de-Sá et al., 2010). Together, these results establish Yrt as a novel multiphosphorylated substrate of aPKC.

aPKC preserves apical membrane integrity through phosphorylation-dependent exclusion of Yrt

To address the functional impact of the aPKC-dependent phosphorylation of Yrt in vivo, we generated transgenic flies expressing either Flag-tagged full-length Yrt (Yrt^{FL}) or the nonphosphorylatable mutant Yrt^{5A} (full-length Yrt carrying S348A, S358A, T379A, S387A, and S392A mutations). Analysis of cuticle integrity revealed that overexpression of Yrt^{FL} had a dominant effect and resulted in the formation of large holes in the ventral epidermis and impairment of head epidermis morphogenesis (Fig. 3, A and B). Although expressed at a level similar to Yrt^{FL} (Fig. 3 E), Yrt^{5A} was associated with a much more dramatic phenotype characterized by epithelial tissue collapse resulting in dispersed grains of cuticle (Fig. 3 C). Expression of Yrt^{5A} phenocopies a complete loss of critical positive regulators of the apical domain, including Crb, Stardust, and aPKC (Tepass et al., 1990; Tepass and Knust, 1993; Harris and Peifer, 2007). This suggests that the Yrt mutant resistant to phosphorylation by aPKC has an enhanced ability to antagonize the apical machinery and, thus, disrupts the integrity of the apical domain. Accordingly, Crb and aPKC expression was severely reduced in most ectodermal cells of embryos expressing Yrt^{5A}, and the lateral proteins Discs large (Dlg) and Yrt (Yrt^{5A}) lined the entire circumference of cells lacking aPKC and Crb (compare Fig. 3, H [arrowheads] with F). Residual Crb and aPKC staining marked the contact point of contracted apexes of cells forming rosettes (Fig. 3 H, arrows). Yrt^{5A} and Dlg invaded these constricted apical domains in stage 12 embryos. In contrast, overexpressed Yrt^{FL} was mostly restricted to the lateral domain along with Dlg at the same stage of embryogenesis (Fig. 3 G). This shows that segregation of lateral and apical proteins and exclusion of Yrt from the apical membrane require phosphorylation of Yrt by aPKC, which neutralizes Yrt activity at the apical membrane. In agreement with this model, reduction of aPKC levels or activity exacerbated the phenotype associated with Yrt overexpression, whereas aPKC overexpression had the opposite effect (Fig. S3, A–L). In addition, expression of the phosphomimetic Yrt^{5D} mutant (S348D, S358D, T379D, S387D, and S392D) had a weaker impact compared with overexpression of Yrt^{FL} and Yrt^{5A}. Yrt^{5D} expression produced mild epithelial morphogenesis defects characterized by the presence of small ventral holes, but development of anterior structures and apical–basal polarity were normal (Fig. 3, D, E, and I). In comparison to Yrt^{FL} and Yrt^{5A}, which were mainly associated with the plasma membrane, Yrt^{5D} showed a more diffuse distribution and accumulated in the cytoplasm (Fig. 3, G–I). This suggests that phosphorylation by aPKC prevents cortical localization of Yrt. Collectively, these results demonstrate that aPKC-dependent phosphorylation of Yrt is a critical event for proper epithelial cell polarization. Specifically, aPKC antagonizes Yrt functions to preserve the integrity of the apical domain and epithelial tissue organization.

Yrt controls apical–basal polarity by limiting aPKC functions

To further explore the physiological outcome of the interaction between Yrt and aPKC, we produced a Yrt mutant protein lacking the FA domain that is required for the interaction with aPKC (referred to as Yrt$^{\Delta FA}$). Yrt$^{\Delta FA}$ was located at both the apical and lateral membranes of ectodermal cells in stage 11 embryos, whereas endogenous Yrt and Yrt^{FL} were restricted to the lateral membrane at this stage of embryogenesis (Fig. 4, A–C).

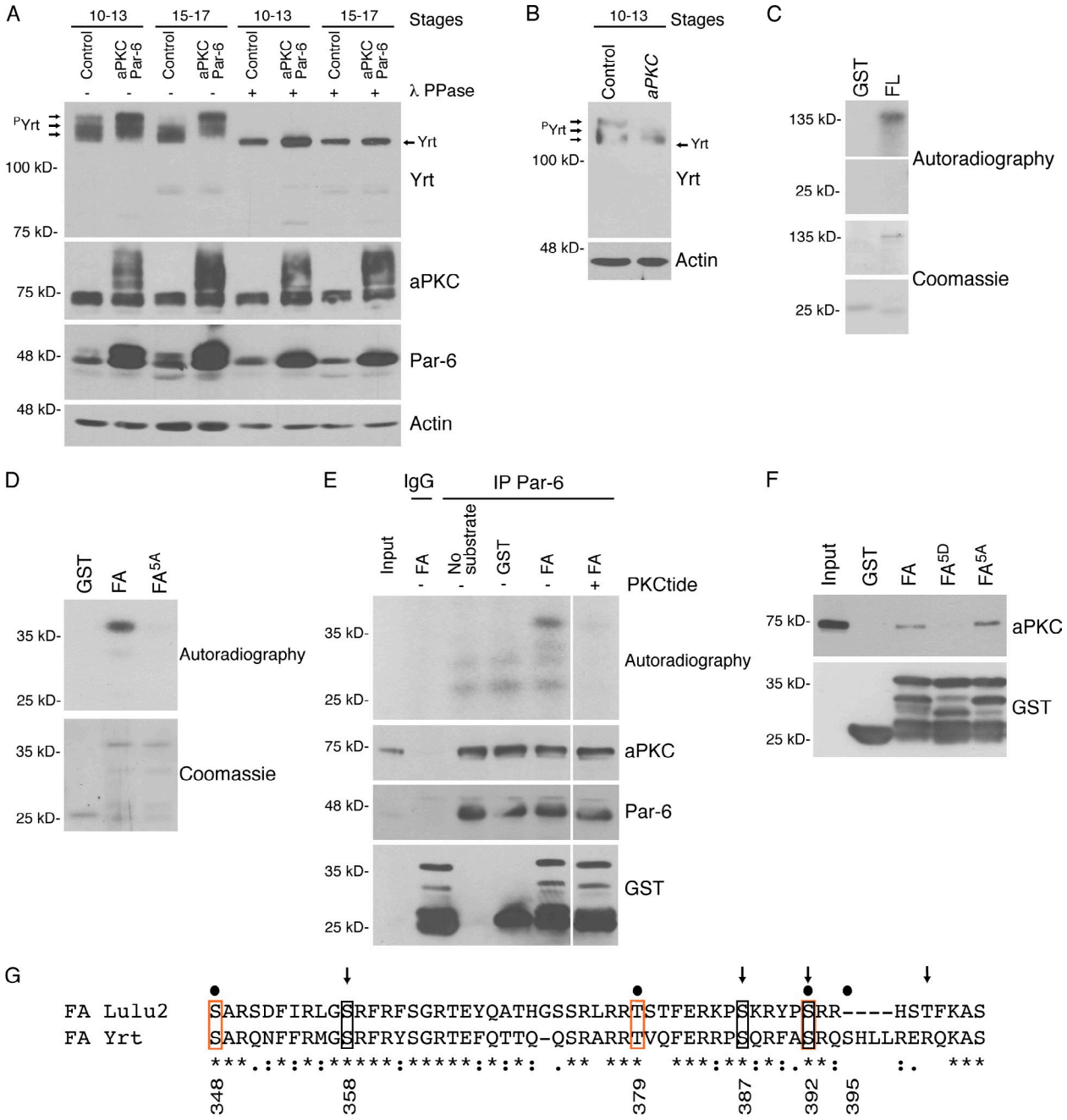

Figure 2. **Yrt is a substrate of aPKC.** (A) Control embryos (*daughterless* [*da*]-*GAL4*) or embryos overexpressing Par-6 and aPKC^{CAAX} (*da-GAL4/UAS–Par-6* and *UAS-aPKC^{CAAX}*) were homogenized at different developmental stages. Samples were treated or not treated with the λ phosphatase (λ PPase) and processed for SDS-PAGE. Western blotting using anti-Yrt antibodies showed the migration profile of Yrt, whereas Actin was used as loading control. (B) Western blot showing the migration profile of Yrt extracted from control (wild type) or *aPKC* maternal and zygotic mutant embryos (we used the allele *aPKC^{psu265}* that encodes a kinase inactive protein; Kim et al., 2009). Actin was used as a loading control. (C and D) Radioactive kinase assays in which purified aPKC was incubated with GST coupled to full-length Yrt (FL; C) or an extended version of the FA domain of Yrt (FA; aa 330–415) and a mutant version of it in which S348, S358, T379, S387, and S392 were mutagenized to A residues (FA^{5A}; D). Proteins were separated on a polyacrylamide gel, which was exposed to monitor protein phosphorylation and then colored with Coomassie blue to control the amount of substrate used in each sample. (E) Anti–Par-6 antibodies were used to immunoprecipitate Par-6 from wild-type embryo extracts (stages 10–13; immunoprecipitate [IP] Par-6), whereas normal guinea pig IgG (IgG) was used as a negative control. GST or GST-FA was added to precipitate along with radiolabeled ATP in the absence or presence of PKCtide, which is a high affinity substrate of aPKC. Proteins were separated by SDS-PAGE, and the gel was exposed to monitor protein phosphorylation. Then, proteins were transferred on a membrane to validate immunoprecipitation of Par-6 and coimmunoprecipitation of aPKC and to monitor the amount of substrate used in each reaction. (F) GST pull-down experiments were performed on wild-type embryo lysates using GST-FA (FA), the nonphosphorylatable GST-FA^{5A} (FA^{5A}), or the phosphomimetic GST-FA^{5D} (FA^{5D}). GST alone was used as a negative control. Western blotting detected pulled down aPKC and monitored the amount of GST or GST fusion proteins used in each experiment. (G) Alignment of the FA domain of mouse Lulu2 and *Drosophila* Yrt. Numbers indicate amino acid positions in the Yrt sequence. Arrows point to amino acids previously shown to be phosphorylated by aPKC in Lulu2 (Nakajima and Tanoue, 2011). Three of these residues are conserved in Yrt (black rectangles). Black circles indicate phosphorylated residues identified by MS in the FA domain of Yrt. Three of these residues are conserved in Lulu2 (orange rectangles). As per ClustalW nomenclature (Larkin et al., 2007), asterisks indicate positions that have fully conserved residues. Colons designate conservation between groups of strongly similar properties, and periods indicate conservation between groups of weakly similar properties.

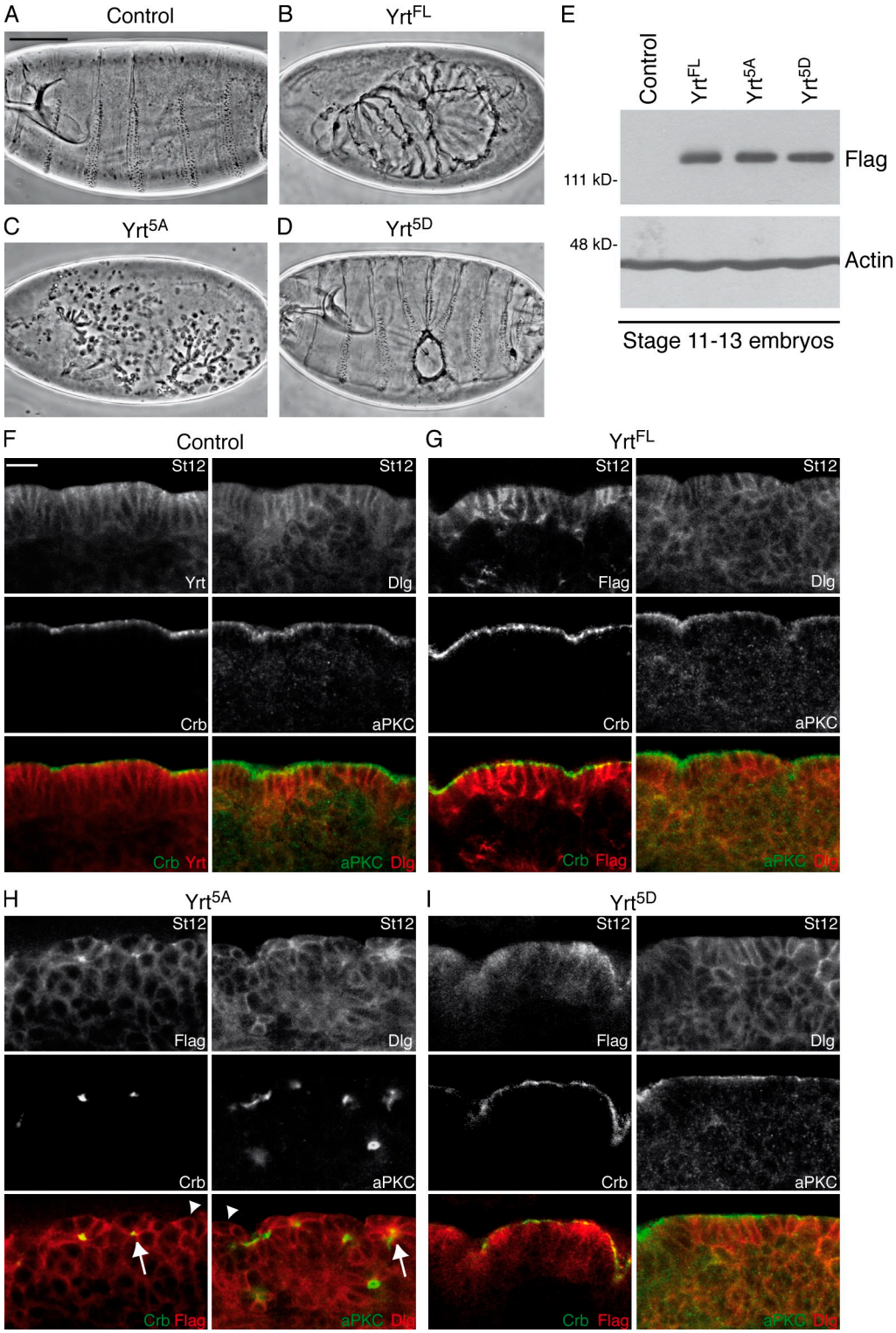

Figure 3. **aPKC-dependent phosphorylation of Yrt is crucial for epithelial cell polarity.** (A–D) Cuticle preparation of embryos of the following genotypes: wild type (A), *da-GAL4/UAS-Flag-yrt*^{FL} (ubiquitous expression of Flag-tagged Yrt^{FL}; B), *da-GAL4/UAS-Flag-yrt*^{5A} (C), and *da-GAL4/UAS-Flag-yrt*^{5D} (D). Bar, 100 μm (also applies to B–D). (E) Western blot using an anti-Flag antibody showing that all constructs were expressed at similar levels. Actin was used as a loading control. (F) Portion of the ventral ectoderm of control (*da-GAL4;* driver line used to express Yrt constructs, this line has a wild-type phenotype) stage 12 (St12) embryos costained with Yrt and Crb (left) or with Dlg and aPKC (right). (G–I) Left images show costaining of Flag and Crb, whereas right images depict costaining of Dlg and aPKC in the ectoderm of an embryo expressing Flag-tagged Yrt^{FL} (G), an embryo expressing Flag-Yrt^{5A} (H), or an embryo expressing Flag-Yrt^{5D} (I). Arrows in H point to cysts of cells with contracted apexes, whereas arrowheads show cells with reduced Crb and aPKC levels. Bar, 10 μm (also applies to G–I).

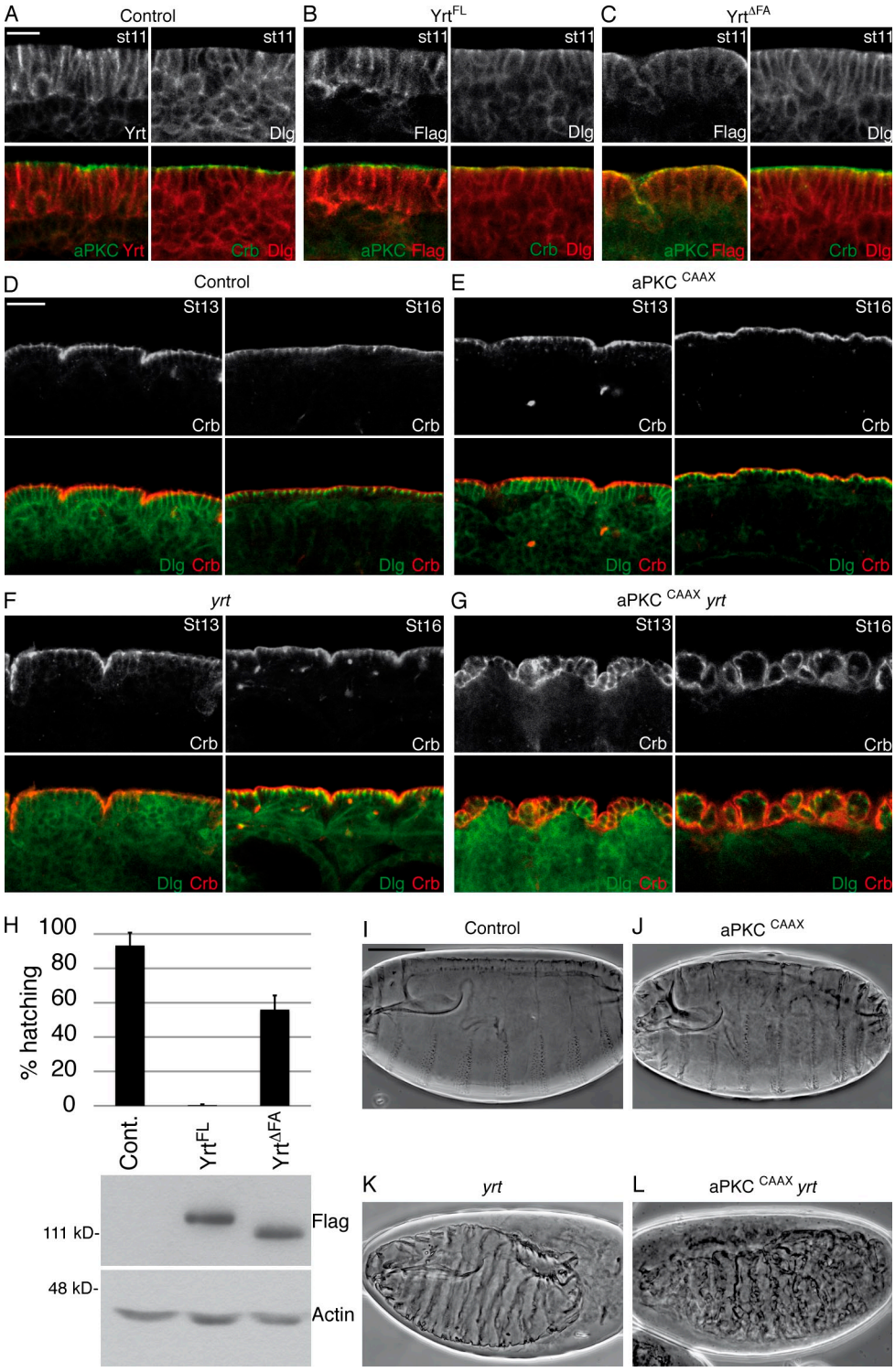

Figure 4. **Yrt limits aPKC-dependent apicalization of epithelial cells.** (A) Portion of the ventral ectoderm of stage 11 control (*da-GAL4*) embryos stained for Yrt and aPKC (left) or Dlg and Crb (right). Bar, 10 µm (also applies to B and C). (B and C) Left images illustrate a portion of the ventral ectoderm costained with Flag and aPKC, whereas right images show a costaining of Dlg and Crb in stage 11 embryos expressing Flag-tagged Yrt^{FL} (B) or embryos expressing Flag-$Yrt^{\Delta FA}$ (C). (D–G) Ventral ectoderm of stage 13 (St13) embryos (left) or ventral epidermis of stage 16 (St16) embryos (right) costained for Dlg and Crb. The embryonic genotypes were *da-GAL4* (D), *UAS-aPKC^{CAAX}; da-GAL4* (ubiquitous expression of membrane-targeted aPKC; E), *yrt^{75a}* (zygotic mutants; F), and *UAS-aPKC^{CAAX}; da-GAL4, yrt^{75a}/yrt^{75a}* (G). Bar, 20 µm (also applies to E–G). (H) Histogram showing the hatching percentage of control (*da-GAL4*) embryos, embryos expressing Yrt^{FL}, or embryos expressing $Yrt^{\Delta FA}$. Error bars represent standard deviation. Below the histogram, a Western blot using an anti-Flag antibody shows that Flag-Yrt^{FL} and Flag-$Yrt^{\Delta FA}$ are expressed at equivalent levels. Blotting for Actin validated equal loading. Cont., control. (I–L) Cuticle preparation of embryos of the following genotypes: *da-GAL4* (I), *UAS-aPKC^{CAAX}; da-GAL4* (J), *yrt^{75a}* (K), and *UAS-aPKC^{CAAX}; da-GAL4, yrt^{75a}/yrt^{75a}* (L). Bar, 100 µm (also applies to J–L).

This is in agreement with our model that aPKC is responsible for the apical exclusion of Yrt normally prevailing in maturing epidermal cells (Laprise et al., 2006), as suggested by our data with Yrt^{5A}. Thereby, our results provide a molecular basis explaining the spatiotemporal dynamics of Yrt previously described (Laprise et al., 2006). Strikingly, although $Yrt^{\Delta FA}$ is ectopically associated with the apical membrane, it had no impact on epithelial cell polarity in contrast to Yrt^{5A}. Indeed, the apical markers aPKC and Crb as well as the lateral protein Dlg were distributed normally in $Yrt^{\Delta FA}$-expressing embryos (Fig. 4 C). This implies that apical Yrt impacts on apical–basal polarity at midembryogenesis primarily by binding to aPKC rather than Crb, which also directly associates with Yrt within the apical domain (Laprise et al., 2006). Moreover, expression of $Yrt^{\Delta FA}$ had a limited impact on embryo survival, whereas expression of Yrt^{FL} is fully lethal (Fig. 4 H). This further suggests that binding to aPKC is a fundamental function of Yrt and proposes that Yrt controls the action of its negative regulator aPKC. Accordingly, although zygotic expression of $aPKC^{CAAX}$ in wild-type embryos did not interfere with epithelial cell polarity, its expression in a *yrt*-sensitized background resulted in a striking apicalization phenotype. The latter was characterized by the expansion of Crb expression territories (Fig. 4, D–G, left) followed by extreme extension of the apical membrane of epidermal cells leading to the formation of inverted cysts toward the end of embryogenesis (i.e., apical membrane facing out; Fig. 4 G, right). Consequently, the larval cuticle, secreted through the apical domain, formed small spheres typical of apicalized epidermal cells (Fig. 4, I–L; Wodarz et al., 1995). The $aPKC^{CAAX}$-induced phenotype in *yrt* mutant embryos mimics polarity defects associated with a strong Crb gain of function or a loss of the lateral protein Lethal (2) giant larvae (Lgl; Wodarz et al., 1995; Bilder et al., 2000). This is consistent with previous studies showing that aPKC favors apical membrane development by enhancing Crb activity through phosphorylation of its cytoplasmic tail (Sotillos et al., 2004) and via inhibition of Lgl functions by dislodging it from the apical membrane (Plant et al., 2003; Hutterer et al., 2004). These data demonstrate that a reduction of Yrt levels allows for aPKC-dependent apicalization of epithelial cells, thereby highlighting Yrt as a critical inhibitor of aPKC-mediated signaling.

Overall, our study establishes that Yrt and aPKC are involved in a reciprocal antagonistic regulatory loop that contributes to segregation and maintenance of discrete membrane domains in epithelial cells and adds complexity to the model of mutual antagonism, leading to apical and lateral membrane domain formation (Fletcher et al., 2012). aPKC phosphorylates several residues in the FA domain of Yrt to weaken their association, thus favoring the apical exclusion of Yrt. Phosphorylation of Yrt is a critical function of aPKC, as a nonphosphorylatable Yrt mutant disrupts the apical domain. The association between Yrt and aPKC also negatively impacts on the function of the latter, thereby conferring to Yrt its ability to maintain apical–basal polarity at midembryogenesis. Therefore, the relative abundance of Yrt and aPKC in their respective membrane domain helps to define a sharp boundary between apical and lateral territories in epithelial cells.

Materials and methods

Molecular biology, DNA cloning, and generation of transgenic lines

DNA fragments were PCR amplified using *Pyrococcus furiosus* DNA polymerase (Agilent Technologies) and subcloned in pGEX-6p-2 or pUASTattB (provided by K. Basler, University of Zurich, Zurich, Switzerland) using the cloning kit (In-Fusion; Takara Bio Inc.; according to the manufacturer's instructions). Positive clones were fully sequenced and transformed in BL21 cells for protein expression (pGEX constructs) or injected in *Drosophila* embryos to generate transgenic lines (pUAS constructs). Injections were performed at BestGene, Inc. Transgenes were inserted with the PhiC31 integrase-mediated transgenesis system using lines carrying an attP docking site (generated by K. Basler's group; Bloomington Stock Center numbers 24485 and 24749). The following transgenic lines were generated: upstream activating sequence (UAS)-3×Flag-Yrt full-length wild type (β isoform [Laprise et al., 2006]; Yrt^{FL}), UAS-3×Flag-$Yrt^{\Delta FA}$ (a mutant version of Yrt lacking the FA domain), UAS-3×Flag-Yrt^{5A} (a nonphosphorylatable version of Yrt; S348A, S358A, T379A, S387A, and S392A), and UAS-3×Flag-Yrt^{5D} (a phosphomimetic version of Yrt; S348D, S358D, T379D, S387D, and S392D).

Drosophila genetics

The *yrt* mutant allele used in this study was yrt^{75a} (Laprise et al., 2006). aPKC (provided by S. Campuzano, Centro de Biología Molecular Severo Ochoa, Madrid, Spain; Sotillos et al., 2004), $aPKC^{CAAX\ WT}$ (Sotillos et al., 2004), $aPKC^{CAAX\ DN}$ (Sotillos et al., 2004), $aPKC^{CAAX\ WT}$, Par-6 (provided by T. Harris, University of Toronto, Toronto, Ontario, Canada; David et al., 2010), full-length Yrt, and Yrt mutant versions were expressed in embryos by crossing the corresponding UAS lines with *da-GAL4* flies at 25 or 29°C. Expression in eyes was driven by *eyeless-GAL4*, and the line y[1] sc[*] v[1]; P{y[+t7.7] v[+t1.8]=TRiP.GL00007}attP2 was used to knockdown aPKC. $aPKC^{CAAX\ WT}$ was expressed in *yrt* mutant embryos by crossing yrt^{75a}, *da-GAL4* flies to UAS-$aPKC^{CAAX\ WT}$; yrt^{75a} flies at 25°C. *aPKC* mutant embryos were obtained from $aPKC^{psu265}$ (Kim et al., 2009) germline clone females, (P{ry[+t7.2]=hsFLP}1, y[1] w[1118]; P{FRT(w^{hs})}G13 (42B), P{ovoD1-18}2R/P{FRT(w^{hs})}G13 (42B), $aPKC^{psu265}$), which were heat shocked three times for 2 h at 37°C as second and third instar larvae and crossed to $aPKC^{psu265}$/CyO males (provided by A. Wodarz, Göttingen University, Göttingen, Germany).

Immunofluorescence

Embryos were dechorionated in 2% sodium hypochlorite for 5 min and heat fixed in 5 ml of E wash (7% NaCl and 0.5% Triton X-100) at 80°C, which was immediately cooled down by the addition of 15 ml of ice-cold E wash. Embryos were then rinsed with PBS and placed in methanol under a heptane phase, devitelinized by strong agitation, and further incubated for 1 h in fresh methanol. Embryos were saturated in NGT (2% normal goat serum and 0.3% Triton X-100 in PBS). Primary antibodies were diluted in NGT and incubated overnight at 4°C under agitation. Primary antibodies used were mouse anti-Dlg (1:10 dilution; clone 4F3; Developmental Studies Hybridoma Bank), rat anti-Crb (1:500; Pellikka et al., 2002), guinea pig anti-Yrt (1:250; Laprise et al., 2006), rabbit anti-aPKC C-20 (1:250; Santa Cruz Biotechnology, Inc.), and mouse anti-Flag (1:250; clone M2; Sigma-Aldrich). Secondary antibodies were conjugated to Cy3 (Jackson ImmunoResearch Laboratories, Inc.), Alexa Fluor 488 (Molecular Probes), or Alexa Fluor 647 (Jackson ImmunoResearch Laboratories, Inc.) and used at a dilution of 1:400 in NGT (1 h at room temperature).

Cuticle preparation

Embryos were dechorionated and mounted in Hoyer's mounting media (prepared by mixing 30 g of gum arabic with 50 ml of distilled water, 200 g chloral hydrate, and 20 ml glycerol at 60°C)/lactic acid (1:1) and incubated at 85°C overnight.

Purification of GST fusion proteins

Protein expression was induced by the addition of 0.1 mM IPTG to liquid bacterial cultures (OD of 0.6 at 600 nm) for 16 h at 16°C under agitation. Protein purification protocol was based on a method described by Frangioni and Neel (1993). Pelleted cells were resuspended in STE buffer (10 mM Tris, pH 8.0, 150 mM NaCl, 1 mM EDTA, 0.1 mM phenylmethylsulfonyl fluoride, 10 µg/ml aprotinin, 10 µg/ml leupeptin, and 0.7 µg/ml pepstatin) containing 100 µg/ml lysozyme for 15 min on ice. DTT and sarcosyl were added to reach a final concentration of 5 mM and 1.5%, respectively. Lysates were then sonicated for 1 min and cleared by centrifugation (10,000 *g* for 5 min at 4°C). Triton X-100 was added to the supernatant to obtain a final concentration of 2.5%. Glutathione–Sepharose beads (GE Healthcare) were added and incubated for 2 h at 4°C. Beads were then washed eight times with ice-cold PBS containing 0.1% Triton

X-100 and stored in storage buffer (50 mM Hepes, pH 7.4, 150 mM NaCl, 5 mM DTT, and 10% glycerol) at −80°C.

Western blotting

Embryos were dechorionated in 2% sodium hypochlorite for 5 min, rinsed with water, homogenized in lysis buffer (50 mM Tris-HCl, pH 7.4, 150 mM NaCl, 1 mM EDTA, 0.75% Nonidet P-40, 0.1 mM sodium orthovanadate, 0.1 mM phenylmethylsulfonyl fluoride, 1 mM NaF, 10 µg/ml aprotinin, 10 µg/ml leupeptin, and 0.7 µg/ml pepstatin), and processed for SDS-PAGE and Western blotting as previously described (Laprise et al., 2002). Primary antibodies used were guinea pig anti-Yrt (1:5,000; Laprise et al., 2006), rabbit anti-aPKC C20 (1:2,000; Santa Cruz Biotechnology, Inc.), mouse anti-Flag (1:2,500; clone M2; Sigma-Aldrich), mouse anti-Actin (1:10,000; clone C4; EMD Millipore), guinea pig anti–Par-6 (1:2,000; Kim et al., 2009), and rabbit anti-GST (1:8,000; provided by J.-Y. Masson, Université Laval, Québec, Québec, Canada). HRP-conjugated secondary antibodies were used at a 1:1,000 dilution. For λ phosphatase assays, embryos were lysed in lysis buffer without phosphatase inhibitors. λ Phosphatase (New England Biolabs, Inc.) was used following the manufacturer's recommendations.

Immunoprecipitation

After dechorionation, embryos from an overnight collection were homogenized in ice-cold lysis buffer (50 mM Tris-HCl, pH 7.4, 150 mM NaCl, 1 mM EDTA, 0.75% Nonidet P-40, 0.1 mM sodium orthovanadate, 0.1 mM phenylmethylsulfonyl fluoride, 1 mM NaF, 10 µg/ml aprotinin, 10 µg/ml leupeptin, and 0.7 µg/ml pepstatin), and cellular debris were removed by centrifugation (13,000 *g* for 10 min at 4°C) followed by a filtration through a 0.45-µm filter unit (EMD Millipore). 3 µg of guinea pig anti-Yrt (Laprise et al., 2006) antibody, guinea pig anti–Par-6 (Kim et al., 2009), or normal guinea pig IgG (Santa Cruz Biotechnology, Inc.) was added to 1 mg embryo lysate and incubated for 1 h at 4°C under agitation. 40 µl protein G–Sepharose beads (GE Healthcare; 50% suspension in lysis buffer) was then added and further incubated for 1 h at 4°C under agitation. Immunocomplexes were harvested by centrifugation and washed five times with lysis buffer, and proteins were eluted with Laemmli buffer.

GST pull-down

Embryos (overnight collection) were homogenized in ice-cold lysis buffer (50 mM Tris-HCl, pH 7.4, 150 mM NaCl, 1 mM EDTA, 1% Triton X-100, 0.1 mM sodium orthovanadate, 0.1 mM phenylmethylsulfonyl fluoride, 1 mM NaF, 10 µg/ml aprotinin, 10 µg/ml leupeptin, and 0.7 µg/ml pepstatin), and lysates were cleared by centrifugation (13,000 *g* for 10 min at 4°C) coupled to a filtration through a 0.45-µm filter unit (EMD Millipore). Lysates (1 mg of proteins) were incubated under agitation with 0.5 µg (5 µg for Fig. 1 B) of GST fusion proteins coupled to glutathione–Sepharose beads (2 h at 4°C). GST loaded on Sepharose beads was used as a negative control. Beads were then washed five times with ice-cold lysis buffer, and proteins were eluted with Laemmli buffer.

Kinase assay

500 ng of purified GST fusion proteins and 50 ng of purified aPKC-ζ (EMD Millipore) or immunoprecipitated aPKC were incubated for 30 min at 30°C in reaction buffer (8 mM MOPS/NaOH, pH 7.0, and 0.02 mM EDTA) in presence of ATP/magnesium cocktail (0.1 mM ATP and 15 mM $MgCl_2$; EMD Millipore) and 2 µCi γ-[^{32}P]ATP (PerkinElmer). Addition of Laemmli buffer stopped the reaction. PKCtide (EMD Millipore) was diluted in water and used at a final concentration of 50 µM.

Sample preparation and MS analysis

A total of 2 µg of substrate and 80 ng aPKC-ζ from a nonradioactive kinase assay were processed as previously described (Bisson et al., 2011). In brief, recombinant Yrt proteins from a 15-µl fraction of the kinase reaction were reduced by adding 60 mM DTT (resuspended in 100 mM NH_4HCO_3, pH 8.0) for 30 min at 55°C and alkylated with 40 mM iodoacetamide for 45 min at room temperature in the dark. Proteins were digested with 20 µg/ml of sequencing grade porcine trypsin (Promega) for 3 h at 37°C, and the reaction was stopped by adding 2 µl of 50% CH_2O_2.

A mass spectrometer (TripleTOF 5600; AB Sciex) equipped with an ion source (NanoSpray III; AB Sciex) and coupled to a nanopump (1200; Agilent Technologies) was used for analyses. Tandem mass spectra were extracted, and charge state was deconvoluted and deisotoped in ProteinPilot version 4.5 (AB Sciex). All MS/MS samples were analyzed using Mascot (Matrix Science). Mascot was set up to search the subset of all *Drosophila* proteins extracted from the UniRef100 (March 2012) database (33,950 entries). Searches were performed with carbamidomethyl (C) set as a fixed modification and deamidation (N and Q), oxidation (M), pyro-Glu (E), phospho-Tyr, and phospho-Ser/Thr set as variable modifications. Trypsin was selected for enzyme digestion with up to two missed cleavages. The peptide and fragment mass tolerances were both set at 0.1 D. MS/MS-based peptide and protein identifications were validated using Scaffold (Proteome Software, Inc.). Peptide identifications confirmed with a >95% confidence (Peptide Prophet algorithm) were accepted and so were protein identifications if they contained at least two identified peptides. The probability of correct phosphorylation site assignment was calculated using the Ascore approach (Beausoleil et al., 2006), via Scaffold PTM (Proteome Software, Inc.).

Determination of hatching percentages

200 newly laid embryos of each genotype were placed on an apple plate. 72 h later, larvae and dead embryos were scored, and the hatching percentage was determined by the ratio of living larvae on the number of larvae plus dead embryos. The experiment was performed four times (800 embryos total for each genotypes).

Image acquisition and processing

Embryos were imaged in Vectashield (Vector Laboratories) with a confocal system (FV1000; Olympus) and FluoView 3.0 (Olympus), using a 40× Apochromat lens with a numerical aperture of 0.90. For cuticle analysis, dead embryos were embedded in Hoyer's medium. Pictures were acquired with MetaVue 7.7.7 (Molecular Devices) linked to a camera (CoolSNAP fx; Photometrics), which was mounted on a microscope (Eclipse 600; Nikon). The lens used was a 20× Plan Fluor with a numerical aperture of 0.50. Fly eyes were observed with a stereomicroscope (Discovery V8; Carl Zeiss; Achromat S 0.63× lens, free working distance of 107 mm) and imaged using a camera (AxioCam ICc1; Carl Zeiss) coupled to the AxioVision 4.7.2 software (Carl Zeiss), which was used to measure eye surface area. All image acquisition was performed at room temperature, and the brightness/contrast tool in Photoshop (Adobe) was used to process images.

Sequence alignment

The FA domains of Yrt and Lulu2 were aligned using ClustalW (Larkin et al., 2007).

Online supplemental material

Fig. S1 shows MS/MS spectra identifying phosphorylated residues in the FA domain of Yrt. Fig. S2 depicts aPKC kinase assays performed on Yrt truncations and mutant versions of it. Fig. S3 shows genetic interactions between *aPKC* and *yrt* in embryos and adult eyes. Online supplemental material is available at http://www.jcb.org/cgi/content/full/jcb.201308032/DC1.

We are grateful to Y. Coulombe and J.-Y. Masson for technical support and to É. Paquet for statistical analysis. We thank A. Wodarz, T. Harris, K. Basler, S. Campuzano, J.-Y. Masson, the Bloomington Drosophila Stock Center, and the Developmental Studies Hybridoma Bank for reagents. Confocal microscopy was performed at the Centre de Recherche du Centre Hospitalier Universitaire–Hôtel-Dieu imaging facility. DNA sequencing was carried out at the Genome Sequencing and Genotyping Platform, and MS analysis was performed at the Proteomics Platform of the Centre Hospitalier Universitaire de Québec Research Centre.

This work was supported by an operating grant from the Canadian Institute of Health Research (CIHR) to P. Laprise (MOP-84249), who is a Fonds de Recherche du Québec-Santé (FRQ-S) Junior 2 investigator. F.J.-M. Chartier was supported by a postdoctoral fellowship from the CIHR. Finally, N. Bisson is a FRQ-S/Quebec Breast Cancer Foundation Junior 1 investigator, and experiments performed in his laboratory were funded by CIHR (MOP-130335).

The authors declare no competing financial interests.

Submitted: 6 August 2013
Accepted: 20 December 2013

References

Baines, A.J. 2006. A FERM-adjacent (FA) region defines a subset of the 4.1 superfamily and is a potential regulator of FERM domain function. *BMC Genomics*. 7:85. http://dx.doi.org/10.1186/1471-2164-7-85

Beausoleil, S.A., J. Villén, S.A. Gerber, J. Rush, and S.P. Gygi. 2006. A probability-based approach for high-throughput protein phosphorylation analysis and site localization. *Nat. Biotechnol.* 24:1285–1292. http://dx.doi.org/10.1038/nbt1240

Betschinger, J., K. Mechtler, and J.A. Knoblich. 2003. The Par complex directs asymmetric cell division by phosphorylating the cytoskeletal protein Lgl. *Nature*. 422:326–330. http://dx.doi.org/10.1038/nature01486

Bilder, D., M. Li, and N. Perrimon. 2000. Cooperative regulation of cell polarity and growth by *Drosophila* tumor suppressors. *Science*. 289:113–116. http://dx.doi.org/10.1126/science.289.5476.113

Bisson, N., D.A. James, G. Ivosev, S.A. Tate, R. Bonner, L. Taylor, and T. Pawson. 2011. Selected reaction monitoring mass spectrometry reveals the dynamics of signaling through the GRB2 adaptor. *Nat. Biotechnol.* 29:653–658. http://dx.doi.org/10.1038/nbt.1905

Chao, T.S., and M. Tao. 1991. Modulation of protein 4.1 binding to inside-out membrane vesicles by phosphorylation. *Biochemistry*. 30:10529–10535. http://dx.doi.org/10.1021/bi00107a023

Danilov, Y.N., R. Fennell, E. Ling, and C.M. Cohen. 1990. Selective modulation of band 4.1 binding to erythrocyte membranes by protein kinase C. *J. Biol. Chem.* 265:2556–2562.

David, D.J., A. Tishkina, and T.J. Harris. 2010. The PAR complex regulates pulsed actomyosin contractions during amnioserosa apical constriction in *Drosophila. Development*. 137:1645–1655. http://dx.doi.org/10.1242/dev.044107

Fletcher, G.C., E.P. Lucas, R. Brain, A. Tournier, and B.J. Thompson. 2012. Positive feedback and mutual antagonism combine to polarize Crumbs in the *Drosophila* follicle cell epithelium. *Curr. Biol.* 22:1116–1122. http://dx.doi.org/10.1016/j.cub.2012.04.020

Frangioni, J.V., and B.G. Neel. 1993. Solubilization and purification of enzymatically active glutathione S-transferase (pGEX) fusion proteins. *Anal. Biochem.* 210:179–187. http://dx.doi.org/10.1006/abio.1993.1170

Harris, T.J., and M. Peifer. 2007. aPKC controls microtubule organization to balance adherens junction symmetry and planar polarity during development. *Dev. Cell*. 12:727–738. http://dx.doi.org/10.1016/j.devcel.2007.02.011

Hoover, K.B., and P.J. Bryant. 2002. *Drosophila* Yurt is a new protein-4.1-like protein required for epithelial morphogenesis. *Dev. Genes Evol.* 212:230–238. http://dx.doi.org/10.1007/s00427-002-0231-6

Hutterer, A., J. Betschinger, M. Petronczki, and J.A. Knoblich. 2004. Sequential roles of Cdc42, Par-6, aPKC, and Lgl in the establishment of epithelial polarity during *Drosophila* embryogenesis. *Dev. Cell*. 6:845–854. http://dx.doi.org/10.1016/j.devcel.2004.05.003

Kim, S., I. Gailite, B. Moussian, S. Luschnig, M. Goette, K. Fricke, M. Honemann-Capito, H. Grubmüller, and A. Wodarz. 2009. Kinase-activity-independent functions of atypical protein kinase C in *Drosophila*. *J. Cell Sci.* 122:3759–3771. http://dx.doi.org/10.1242/jcs.052514

Krahn, M.P., J. Bückers, L. Kastrup, and A. Wodarz. 2010. Formation of a Bazooka–Stardust complex is essential for plasma membrane polarity in epithelia. *J. Cell Biol.* 190:751–760. http://dx.doi.org/10.1083/jcb.201006029

Laprise, P., P. Chailler, M. Houde, J.F. Beaulieu, M.J. Boucher, and N. Rivard. 2002. Phosphatidylinositol 3-kinase controls human intestinal epithelial cell differentiation by promoting adherens junction assembly and p38 MAPK activation. *J. Biol. Chem.* 277:8226–8234. http://dx.doi.org/10.1074/jbc.M110235200

Laprise, P., S. Beronja, N.F. Silva-Gagliardi, M. Pellikka, A.M. Jensen, C.J. McGlade, and U. Tepass. 2006. The FERM protein Yurt is a negative regulatory component of the Crumbs complex that controls epithelial polarity and apical membrane size. *Dev. Cell*. 11:363–374. http://dx.doi.org/10.1016/j.devcel.2006.06.001

Laprise, P., K.M. Lau, K.P. Harris, N.F. Silva-Gagliardi, S.M. Paul, S. Beronja, G.J. Beitel, C.J. McGlade, and U. Tepass. 2009. Yurt, Coracle, Neurexin IV and the Na(+),K(+)-ATPase form a novel group of epithelial polarity proteins. *Nature*. 459:1141–1145. http://dx.doi.org/10.1038/nature08067

Larkin, M.A., G. Blackshields, N.P. Brown, R. Chenna, P.A. McGettigan, H. McWilliam, F. Valentin, I.M. Wallace, A. Wilm, R. Lopez, et al. 2007. Clustal W and Clustal X version 2.0. *Bioinformatics*. 23:2947–2948. http://dx.doi.org/10.1093/bioinformatics/btm404

Manno, S., Y. Takakuwa, and N. Mohandas. 2005. Modulation of erythrocyte membrane mechanical function by protein 4.1 phosphorylation. *J. Biol. Chem.* 280:7581–7587. http://dx.doi.org/10.1074/jbc.M410650200

Morais-de-Sá, E., V. Mirouse, and D. St Johnston. 2010. aPKC phosphorylation of Bazooka defines the apical/lateral border in *Drosophila* epithelial cells. *Cell*. 141:509–523. http://dx.doi.org/10.1016/j.cell.2010.02.040

Nakajima, H., and T. Tanoue. 2011. Lulu2 regulates the circumferential actomyosin tensile system in epithelial cells through p114RhoGEF. *J. Cell Biol.* 195:245–261. http://dx.doi.org/10.1083/jcb.201104118

Pellikka, M., G. Tanentzapf, M. Pinto, C. Smith, C.J. McGlade, D.F. Ready, and U. Tepass. 2002. Crumbs, the *Drosophila* homologue of human CRB1/RP12, is essential for photoreceptor morphogenesis. *Nature*. 416:143–149. http://dx.doi.org/10.1038/nature721

Plant, P.J., J.P. Fawcett, D.C. Lin, A.D. Holdorf, K. Binns, S. Kulkarni, and T. Pawson. 2003. A polarity complex of mPar-6 and atypical PKC binds, phosphorylates and regulates mammalian Lgl. *Nat. Cell Biol.* 5:301–308. http://dx.doi.org/10.1038/ncb948

Sotillos, S., M.T. Díaz-Meco, E. Caminero, J. Moscat, and S. Campuzano. 2004. DaPKC-dependent phosphorylation of Crumbs is required for epithelial cell polarity in *Drosophila*. *J. Cell Biol.* 166:549–557. http://dx.doi.org/10.1083/jcb.200311031

Tepass, U. 2009. FERM proteins in animal morphogenesis. *Curr. Opin. Genet. Dev.* 19:357–367. http://dx.doi.org/10.1016/j.gde.2009.05.006

Tepass, U., and E. Knust. 1993. Crumbs and stardust act in a genetic pathway that controls the organization of epithelia in *Drosophila melanogaster*. *Dev. Biol.* 159:311–326. http://dx.doi.org/10.1006/dbio.1993.1243

Tepass, U., C. Theres, and E. Knust. 1990. *crumbs* encodes an EGF-like protein expressed on apical membranes of *Drosophila* epithelial cells and required for organization of epithelia. *Cell*. 61:787–799. http://dx.doi.org/10.1016/0092-8674(90)90189-L

Walther, R.F., and F. Pichaud. 2010. Crumbs/DaPKC-dependent apical exclusion of Bazooka promotes photoreceptor polarity remodeling. *Curr. Biol.* 20:1065–1074. http://dx.doi.org/10.1016/j.cub.2010.04.049

Wodarz, A., U. Hinz, M. Engelbert, and E. Knust. 1995. Expression of crumbs confers apical character on plasma membrane domains of ectodermal epithelia of *Drosophila*. *Cell*. 82:67–76. http://dx.doi.org/10.1016/0092-8674(95)90053-5

Yamanaka, T., Y. Horikoshi, Y. Sugiyama, C. Ishiyama, A. Suzuki, T. Hirose, A. Iwamatsu, A. Shinohara, and S. Ohno. 2003. Mammalian Lgl forms a protein complex with PAR-6 and aPKC independently of PAR-3 to regulate epithelial cell polarity. *Curr. Biol.* 13:734–743. http://dx.doi.org/10.1016/S0960-9822(03)00244-6